

RESIDUAL CONNECTIONS ENCOURAGE ITERATIVE INFERENCE

Stanisław Jastrzebski^{*†}, Devansh Arpit^{*‡}, Nicolas Ballas[‡], Vikas Verma[§]
Tong Che[‡], Yoshua Bengio^{‡¶}

ABSTRACT

Residual networks (Resnets) have become a prominent architecture in deep learning. However, a comprehensive understanding of Resnets is still a topic of ongoing research. A recent view argues that Resnets perform iterative refinement of features. We attempt to further expose properties of this aspect. To this end, we study Resnets both analytically and empirically. We formalize the notion of iterative refinement in Resnets by showing that residual architectures naturally encourage features to move along the negative gradient of loss during the feedforward phase. In addition, our empirical analysis suggests that Resnets are able to perform both representation learning and iterative refinement. In general, a Resnet block tends to concentrate representation learning behavior in the first few layers while higher layers perform iterative refinement of features. Finally we observe that sharing residual layers naively leads to representation explosion and hurts generalization performance, and show that simple existing strategies can help alleviating this problem.

1 INTRODUCTION

Traditionally, deep neural network architectures (eg. VGG [Simonyan & Zisserman \(2014\)](#), alexnet [Krizhevsky et al. \(2012\)](#), etc.) have been compositional in nature, meaning a hidden layer applies an affine transformation followed by non-linearity, with a different transformation at each layer. However, a major problem with deep architectures has been that of vanishing and exploding gradients. To address this problem, solutions like better activations (ReLU [Nair & Hinton \(2010\)](#)), weight initialization methods [Glorot & Bengio \(2010\)](#); [He et al. \(2015\)](#) and normalization methods [Ioffe & Szegedy \(2015\)](#); [Arpit et al. \(2016\)](#) have been proposed. Nonetheless, training compositional networks deeper than 15 – 20 layers remains a challenging task.

Recently, residual networks (Resnets [He et al. \(2016a\)](#)) were introduced to tackle these issues and are considered a breakthrough in deep learning because of their ability to learn very deep networks and achieve state-of-the-art performance. Besides this, performance of Resnets are generally found to remain largely unaffected by removing individual residual blocks or shuffling adjacent blocks [Veit et al. \(2016\)](#). These attributes of Resnets stem from the fact that residual blocks transform representations additively instead of compositionally (like traditional deep networks). This additive framework along with the aforementioned attributes has given rise to two school of thoughts about Resnets– the ensemble view where they are thought to learn an exponential ensemble of shallower models [Veit et al. \(2016\)](#), and the unrolled iterative estimation view [Liao & Poggio \(2016\)](#); [Greff et al. \(2016\)](#), where Resnet layers are thought to iteratively refine representations instead of learning new ones.

While the success of Resnets may be attributed partly to both these views, our work takes steps towards achieving a deeper understanding of Resnets in terms of its iterative feature refinement perspective. Our contributions are as follows:

^{*}First two authors contributed equally

[†]Jagiellonian University

[‡]MILA, Université de Montréal

[§]Aalto University

[¶]CIFAR Senior Fellow

1. We study Resnets analytically and provide a formal view of iterative feature refinement using Taylor’s expansion, showing that for any loss function, a residual layer naturally encourages representations to move along the negative gradient of the loss with respect to hidden representations. Each residual layer is therefore encouraged to take a gradient step in order to minimize the loss in the hidden representation space. We empirically confirm this by measuring the cosine between hidden representations and gradient of loss with respect to the hidden representations.

2. We empirically observe that Resnet layers can perform both representation learning and iterative feature refinement. Specifically in Resnets, lower residual blocks learn to perform representation learning, meaning that they change representations significantly and removing these layer can sometime drastically hurts prediction performance. The higher blocks on the other hand essentially learn to perform iterative inference, minimizing the loss function by moving along the negative gradient direction. In the presence of shortcut connections¹, representation learning is dominantly performed by the compositional layers and most of residual blocks tend to perform iterative feature refinement. We also show that unrolling the top blocks (performing iterative inference) at test time, improves test accuracy of Resnet models.

3. The iterative refinement view suggests that deep network models can potentially leverage intensive parameter sharing for the layer performing iterative inference. But sharing large number of residual blocks without loss of performance has not been successfully achieved yet. Towards this end, we study the applicability of sharing residual blocks in Resnets given their iterative feature refinement view and expose reasons for the failure of sharing in Resnets and investigate a preliminary fix for this problem.

2 BACKGROUND AND RELATED WORK

Residual Networks and their analysis:

Recently, several papers have investigated the behavior of Resnets (He et al., 2016a). In (Veit et al., 2016; Littwin & Wolf, 2016), authors argue that Resnets are an ensemble of relatively shallow networks. This is based on the unraveled view of Resnets where there exist exponential number of paths between the input and prediction layer. Further, observations like shuffling and dropping of residual blocks do not affect performance significantly also support this claim. Other works discuss the possibility that residual networks are approximating recurrent network like models (Liao & Poggio, 2016; Greff et al., 2016). This view is in part supported by the observation that the mathematical formulation of Resnets bares similarity to LSTM (Hochreiter & Schmidhuber, 1997), and that successive layers cooperate and preserve the feature identity. Resnets have also been studied from the perspective of boosting theory Huang et al. (2017). In this work the authors propose to learn Resnets in a layerwise manner using a local classifier.

Our work bears critical differences compared with the aforementioned studies. Most importantly we focus on a precise definition of iterative inference. In particular, we show that a residual block approximate a gradient descent step in the activation space. Our work can also be seen as relating the gap the boosting and iterative inference interpretations since having a residual block whose output is aligned with negative gradient of loss is similar to how gradient boosting models work.

Iterative refinement and weight sharing:

Humans frequently perform predictions with iterative refinement based on the level of difficulty of the task at hand. A leading hypothesis regarding the nature of information processing that happens in the visual cortex is that it performs fast feedforward inference (Thorpe et al., 1996) for easy stimuli or when quick response time is needed, and performs iterative refinement of prediction for complex stimuli (Vanmarcke et al., 2016). The latter is thought to be done by lateral connections within individual layers in the brain that iteratively act upon the current state of the layer to update it. This mechanism allows the brain to make fine grained predictions on complex tasks. A characteristic attribute of this mechanism is the recursive application of the lateral connections which can be thought of as shared weights in a recurrent model. The above views suggest that it is desirable to

¹A shortcut connection is a convolution layer between residual blocks useful for changing the hidden space dimension (see He et al. (2016a) for instance).

have deep network models that perform parameter sharing in order to make the iterative inference view complete.

3 RESNET ANALYSIS

In this section we study the properties of representations that residual blocks tend to learn, as a result of being additive in nature, in contrast to traditional compositional networks. Specifically, we consider Resnet architectures (see figure 1) where the first hidden layer is a convolution layer, which is followed by L residual blocks which may or may not have *shortcut* connections in between residual layers.

A residual layer applied on a representation \mathbf{h}_i transforms the representation as,

$$\mathbf{h}_{i+1} = \mathbf{h}_i + F_i(\mathbf{h}_i) \quad (1)$$

Consider L such residual blocks stacked on top of each other followed by a loss function. Then, we can Taylor expand any given loss function \mathcal{L} recursively as,

$$\mathcal{L}(\mathbf{h}_L) = \mathcal{L}(\mathbf{h}_{L-1} + F_{L-1}(\mathbf{h}_{L-1})) \quad (2)$$

$$= \mathcal{L}(\mathbf{h}_{L-1}) + F_{L-1}(\mathbf{h}_{L-1}) \cdot \frac{\partial \mathcal{L}(\mathbf{h}_{L-1})}{\partial \mathbf{h}_{L-1}} \quad (3)$$

$$+ \mathcal{O}(F_{L-1}^2(\mathbf{h}_{L-1}))$$

$$= \mathcal{L}(\mathbf{h}_i) + \sum_{j=i}^{L-1} F_j(\mathbf{h}_j) \cdot \frac{\partial \mathcal{L}(\mathbf{h}_j)}{\partial \mathbf{h}_j} + \mathcal{O}(F_j^2(\mathbf{h}_j)) \quad (4)$$

Notice we have explicitly only written the first order terms of each expansion. The rest of the terms are absorbed in the higher order terms in $\mathcal{O}(\cdot)$. Furthermore, the first order term is a good approximation when the magnitude of F_j is small enough. In other cases, the higher order terms come into effect as well.

Thus in part, the loss equivalently minimizes the dot product between $F(\mathbf{h}_i)$ and $\frac{\partial \mathcal{L}(\mathbf{h}_i)}{\partial \mathbf{h}_i}$, which can be achieved by making $F(\mathbf{h}_i)$ point in the opposite half space to that of $\frac{\partial \mathcal{L}(\mathbf{h}_i)}{\partial \mathbf{h}_i}$. In other words,

$\mathbf{h}_i + F(\mathbf{h}_i)$ approximately moves \mathbf{h}_i in the same half space as that of $-\frac{\partial \mathcal{L}(\mathbf{h}_i)}{\partial \mathbf{h}_i}$. The overall training criteria can then be seen as approximately minimizing the cosine loss between these 2 terms along a path in the \mathbf{h} space between \mathbf{h}_i and \mathbf{h}_L such that loss gradually reduces as we take steps from \mathbf{h}_i to \mathbf{h}_L . One can therefore also expect accuracy to increase gradually as the representations go through residual layers.

4 EMPIRICAL ANALYSIS

Experiments are performed on CIFAR-10 (Krizhevsky & Hinton, 2009) and CIFAR-100 (see appendix) using the original Resnet architecture He et al. (2016b) and two other architectures that we introduce for the purpose of our analysis (described below). Our main goal is to validate that residual networks perform iterative refinement as discussed above, showing its various consequences. Specifically, we set out to empirically answer the following questions:

- Do residual blocks in Resnets behave similar to each other or is there a distinction between blocks that perform iterative refinement vs. representation learning?
- Is the cosine between $\frac{\partial \mathcal{L}(\mathbf{h}_i)}{\partial \mathbf{h}_i}$ and $F_i(\mathbf{h}_i)$ negative in residual networks?
- What kind of samples do residual blocks target?
- What happens when layers are shared in Resnets?

Resnet architectures: We use the following four architectures for our analysis:

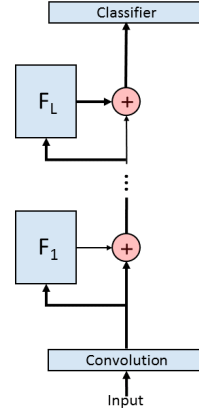


Figure 1: A typical residual network architecture.

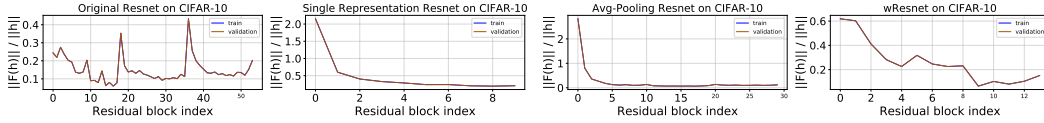


Figure 2: Average ratio of ℓ^2 norm of output of residual block to the norm of the input of residual block for (left to right) original Resnet, single representation Resnet, avg-pooling Resnet, and wideResnet on CIFAR-10. (Train and validation curves are overlapping.)

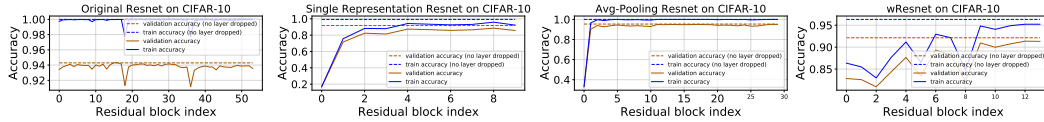


Figure 3: Final prediction accuracy when individual residual blocks are dropped for (left to right) original Resnet, single representation Resnet, avg-pooling Resnet, and wideResnet on CIFAR-10.

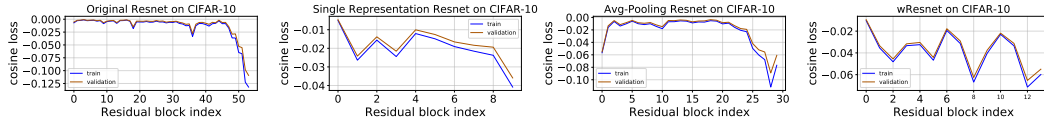


Figure 4: Average cosine loss between residual block $F(\mathbf{h}_i)$ and $\frac{\partial \mathcal{L}(\mathbf{h}_i)}{\partial \mathbf{h}_i}$ for (left to right) original Resnet, single representation Resnet, avg-pooling Resnet, and wideResnet on CIFAR-10.

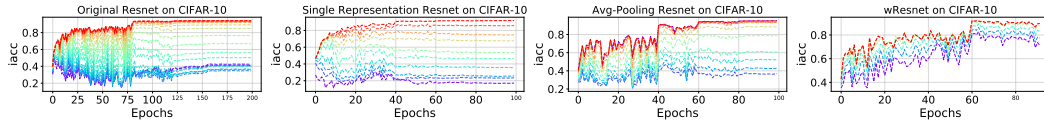


Figure 5: Prediction accuracy when plugging classifier after hidden states in the last stage of Resnets (if any) during training for (left to right) original Resnet, single representation Resnet, avg-pooling Resnet, and wideResnet on CIFAR-10. (Blue to red spectrum denotes lower to higher residual blocks)

1. Original Resnet-110 architecture: This is the same architecture as used in [He et al. \(2016b\)](#) starting with a 3×3 convolution layer with 16 filters followed by 54 residual blocks in three different stages (of 18 blocks each with 16, 32 and 64 filters respectively) each separated by a shortcut connections (1×1 convolution layers that allow change in the hidden space dimensionality) inserted after the 18th and 36th residual blocks such that the 3 stages have hidden space of height-width 32×32 , 16×16 and 8×8 . The model has a total of 1,742,762 parameters.

2. Single representation Resnet: This architecture starts with a 3×3 convolution layer with 100 filters. This is followed by 10 residual blocks such that all hidden representations have the same height and width of 32×32 and 100 filters are used in all the convolution layers in residual blocks as well.

3. Avg-pooling Resnet: This architecture repeats the residual blocks of the single representation Resnet (described above) three times such that there is a 2×2 average pooling layer after each set of 10 residual blocks that reduces the height and width after each stage by half. Also, in contrast to single representation architecture, it uses 150 filters in all convolution layers. This is followed by the classification block as in the single representation Resnet. It has 12,201,310 parameters. We call this architecture avg-pooling architecture. We also ran experiments with max pooling instead of average pooling but do not report results because they were similar except that max pool acts more non-linearly compared with average pooling, and hence the metrics from max pooling are more similar to those from original resnet.

4. Wide Resnet: This architecture starts with a 3×3 convolution layer followed by 3 stages of four residual blocks with 160, 320 and 640 number of filters respectively, and 3×3 kernel size in all convolution layers. This model has a total of 45,732,842 parameters.

Experimental details: For all architectures, we use *He-normal* weight initialization as suggested in He et al. (2015), and biases are initialized to 0. For residual blocks, we use BatchNorm→ReLU→Conv→BatchNorm→ReLU→Conv as suggested in He et al. (2016b). The classifier is composed of the following elements: BatchNorm→ReLU→AveragePool(8,8)→Flatten→Fully-Connected-Layer(#classes)→Softmax. This model has 1,829,210 parameters. For all experiments for single representation and pooling Resnet architectures, we use SGD with momentum 0.9 and train for 200 epochs and 100 epochs (respectively) with learning rate 0.1 until epoch 40, 0.02 until 60, 0.004 until 80 and 0.0008 afterwards. For the original Resnet we use SGD with momentum 0.9 and train for 300 epochs with learning rate 0.1 until epoch 80, 0.01 until 120, 0.001 until 200, 0.00001 until 240 and 0.000011 afterwards. We use data augmentation (horizontal flipping and translation) during training of all architectures. For the wide Resnet architecture, we train the model with with learning rate 0.1 until epoch 60 and 0.02 until 100 epochs.

Note: All experiments on CIFAR-100 are reported in the appendix. In addition, we also record the metrics reported in sections 4.1 and 4.2 and plot them as a function of epochs (shown in the appendix due to space limitations). The conclusions are similar to what is reported below.

4.1 REPRESENTATION LEARNING VS. FEATURE REFINEMENT

In this section, we are interested in investigating the behavior of residual layers in terms of representation learning vs. refinement of features. To this end, we perform the following experiments.

1. ℓ^2 ratio $\|F_i(\mathbf{h}_i)\|_2/\|\mathbf{h}_i\|_2$: A residual block $F_i(\cdot)$ transforms representation as $\mathbf{h}_{i+1} = \mathbf{h}_i + F_i(\mathbf{h}_i)$. For every such block in a Resnet, we measure the ℓ^2 ratio of $\|F_i(\mathbf{h}_i)\|_2/\|\mathbf{h}_i\|_2$ averaged across samples. This ratio directly shows how significantly $F_i(\cdot)$ changes the representation \mathbf{h}_i ; a large change implies more representation learning while a small change implies feature refinement. Figure 2 shows the ℓ^2 ratio for CIFAR-10 on train and validation sets. For single representation Resnet and pooling Resnet, the first few residual blocks (especially the first residual block) changes representations significantly (up to twice the norm of the original representation), while the rest of the higher blocks are relatively much less significant and this effect is monotonic as we go to higher blocks. However this effect is not as drastic in the original Resnet and wide Resnet architectures which have two 1×1 (shortcut) convolution layers, thus adding up to a total of 3 convolution layers in the main path of the residual network (notice there exists only one convolution layer in the main path for the other two architectures). This suggests that residual blocks in general tend to learn to refine features but in the case when the network lacks enough compositional layers in the main path, the lower residual blocks are forced to change representations significantly, as a proxy for the absence of compositional layers.

2. Effect of dropping residual layer on accuracy: We drop individual residual blocks from trained Resnets and make predictions using the rest of network on validation set. This analysis shows the significance of individual residual blocks towards the final accuracy that is achieved using all the residual blocks. Note, dropping individual residual blocks is possible because adjacent blocks operate in the same feature space. Figure 3 shows the result of dropping individual residual blocks. As one would expect given above analysis, dropping the first few residual layers (especially the first) for single representation Resnet and pooling Resnet leads to catastrophic performance drop while dropping most of the higher residual layers have minimal effect on performance. On the other hand, performance drops are not drastic for the original Resnet and wide Resnet architecture. This is in line with the explanation given in the ℓ^2 ratio experiments above.

In another set of experiments, we measure validation accuracy after individual residual block during the training process. This set of experiments is achieved by plugging the classifier right after each residual block in the last stage of hidden representation (i.e., after the last shortcut connection, if any). This is shown in figure 5. The figures show that accuracy increases very gradually when adding more residual blocks in the last stage of all architectures.

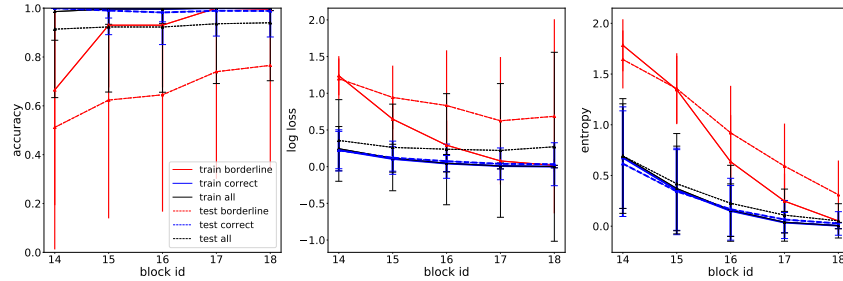


Figure 6: Accuracy, loss and entropy for last 5 blocks of Resnet-110. Performance on *borderline* examples improves at the expense of performance (loss) of already correctly classified points (*correct*). This happens because last block output is encouraged by training to be negatively correlated (around -0.1 cosine) with gradient of the loss.

4.2 COSINE LOSS OF RESIDUAL BLOCKS

We use insights from the Taylor’s expansion analysis above and compute the cosine loss

$\frac{F_i(\mathbf{h}_i) \cdot \frac{\partial \mathcal{L}(\mathbf{h}_i)}{\partial \mathbf{h}_i}}{\|F_i(\mathbf{h}_i)\|_2 \|\frac{\partial \mathcal{L}(\mathbf{h}_i)}{\partial \mathbf{h}_i}\|_2}$. A negative cosine loss and small $F_i(\cdot)$ together suggest that $F_i(\cdot)$ is refining

features by moving them in the half space of $-\frac{\partial \mathcal{L}(\mathbf{h}_i)}{\partial \mathbf{h}_i}$, thus reducing the loss value for the corresponding data samples. Figure 4 shows the cosine loss for CIFAR-10 on train and validation sets. These figures show that cosine loss is consistently negative for all residual blocks but especially for the higher residual blocks. Also, notice for deeper architectures (original Resnet and pooling Resnet), the higher blocks achieve more negative cosine loss and are thus more iterative in nature. Further, since the higher residual blocks make smaller changes to representation (figure 2), the first order Taylor’s term becomes dominant and hence these blocks effectively move samples in the half space of the negative cosine loss thus reducing loss value of prediction. This result formalizes the sense in which residual blocks perform iterative refinement of features— move representations in the half space of $-\frac{\partial \mathcal{L}(\mathbf{h}_i)}{\partial \mathbf{h}_i}$.

4.3 BORDERLINE EXAMPLES

Since individual residual blocks in general lead to small improvements in performance, it is worth identifying qualitatively what kind of samples they constitute. Intuitively, since these layers move representations minimally (as shown by above analysis), the samples that lead to these minor accuracy jump should be near the decision boundary but getting misclassified by a slight margin. To confirm this intuition, we first define *borderline* samples as examples with probability margin below 10% as measured by some non-final block (by plugging the classifier right after the representation that we get using this residual block). Then using the plugged classifier we look at how loss, accuracy and entropy over these samples evolves over last 5 blocks of the network. Figure 6 shows these samples for Resnet110 on CIFAR-10 test and train set. Clearly for every hidden representation, a significant chunk of *borderline* examples get corrected by the residual blocks above it. This exposes the qualitative nature of samples that these feature refinement layers focus on, which is further reinforced by the fact that entropy decreases for all considered subsets. We also note that while train loss drops uniformly across layers, test sets loss *increases* after last block. Correcting this phenomenon could lead to improved generalization in Resnets, which we leave for future work.

4.4 UNROLLING RESIDUAL NETWORK

The experiments so far suggest that higher residual layers learn to perform iterative refinement of features. However, a fundamental requirement for a procedure to be truly iterative is to apply the same function. In this section we explore what happens when we unroll the last block of a trained residual network for more steps than it was trained for. Our main insight is that because cosine loss is negative also on test distribution (in all runs we observe negative cosine loss on both train and test

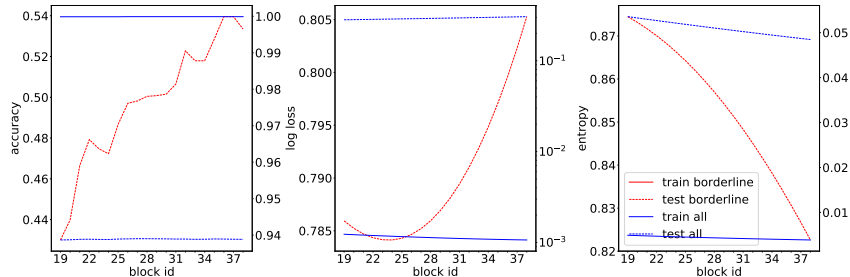


Figure 7: Accuracy, loss and entropy for last 5 blocks of Resnet-110 unrolled for 20 *additional* steps (with appropriate scaling). *Borderline* examples are corrected and overall performance slightly improves. Note different scales for train and test. Curves are averaged over 4 runs of Resnet-110.

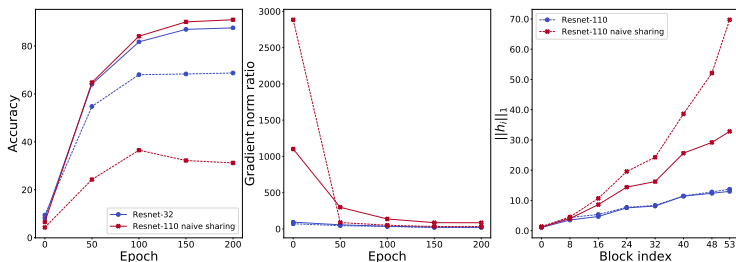


Figure 8: Resnet-110 with naively shared top 13 layers of each block compared with unshared Resnet-32. Left plot present training and validation curves, shared Resnet-110 heavily overfits. In the right plot we track gradient norm ratio between first block in first and last stage of resnet (i.e. $r = \|\frac{\partial L}{\partial h_1}\| / \|\frac{\partial L}{\partial h_{1+2n}}\|$). Significantly larger ratio in the naive sharing model suggests, that the overfitting is caused by early layers dominating learning.

set), it should continue to refine examples within some neighbourhood, and help correct prediction of samples.

We focus first on the same model as discussed in previous section, Resnet-110, and unroll the last residual block for 20 extra steps². Figure 7 shows again evolution of accuracy of three groups of examples: *borderline* examples, *already correctly classified* and the whole dataset. There are on average 51 borderline examples in test set³, on which performance is improved from 43% to 53%, which yields overall slight improvement in accuracy on test set. At the same time loss on test set slightly increases, which can be explained by decreased confidence of prediction on already correctly predicted examples. Loss on train set improved uniformly from 0.0012 to 0.001 (all results are averaged over 4 seeds). We observe described behavior to be generally consistent across Resnets with different number of blocks (32, 38, 56, 110). To summarize, unrolling residual network to more steps than trained on improves both loss and accuracy on train set, and accuracy on test set. Similar behavior can be observed in the last blocks of Resnet (as described in the previous section).

4.5 SHARING RESIDUAL LAYERS

Given the iterative inference view, we now study the effects of sharing residual blocks. Contrary to (Liao & Poggio, 2016) we observe that naively sharing the higher (iterative refinement) residual blocks of a Resnets in general leads to overfitting⁴ (especially for deeper Resnets). In particular, reducing the number of parameters in Resnet-110 (by sharing top 13 blocks in each stage) leads to 91.2% training accuracy on CIFAR-100, below that of unshared Resnet-110 (98.74%) but sig-

²We add scaling factor so that overall change in ℓ^2 norm of h is on average no larger than approximately 2%.

³All examples from train set have confident predictions by last block in the residual network.

⁴(Liao & Poggio, 2016) compared shallow Resnets with shared network having more residual blocks.

Model	CIFAR10	CIFAR100	Parameters
Resnet-32	1.53 / 7.14	12.62 / 30.08	467k-473k
Resnet-38	1.20 / 6.99	10.04 / 29.66	565k-571k
Resnet-110-UBN	0.63 / 6.62	7.75 / 29.94	570k-576k
Resnet-146-UBN	0.68 / 6.82	7.21 / 29.49	573k-579k
Resnet-182-UBN	0.48 / 6.97	6.42 / 29.33	576k-581k
Resnet-56	0.58 / 6.53	5.19 / 28.99	857k-863k
Resnet-110	0.22 / 6.13	1.26 / 27.54	1734k-1740k

Table 1: Train and test error of ResNet sharing top layers blocks (while using unshared both statistics and β, γ in Batch Normalization) compared to baseline ResNet of varying depth. Runs are repeated 4 times. Training ResNet with unrolled layers can bring additional gain of 0.3%, while adding marginal amount of extra parameters.

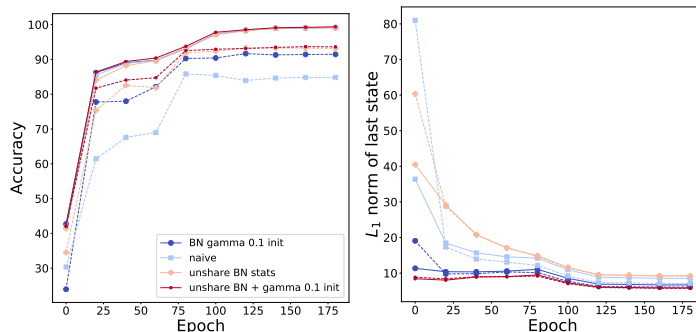


Figure 9: Ablation study of different strategies to remedy sharing leading to overfitting phenomenon in Residual Networks. Left figure shows effect on training and test accuracy. Right figure studies norm explosion. All components are important, but it is most crucial to unshare BN statistics.

nificantly more than Resnet-32 (87.38%). Although Resnet-110 with shared parameters has worse validation error as Fig. 8 report.

Looking at the network naively sharing top layers, we observe that sharing layers make the layer activations explode during the forward propagation at initialization due to the repeated application of the same operation (Fig 8, right). Consequently the norm of the gradients also explodes at initialization (Fig. 8, center). While the Resnets network is able to cope from this phenomenon from an optimization perspective, this initial gradient explosion impacts its generalization capability (Fig. 9).

To address this generalization issue, we introduce a variant of recurrent batch normalization (Cooijmans et al., 2016), which proposes to initialize γ to 0.1 and unshare statistics for every step. On top of this strategy, we also unshare γ and β parameters. Tab. 1 shows that using our strategy alleviates explosion problem and leads to small improvement over baseline with similar number of parameters. We also perform an ablation to study, see figure. 9 (left), which show that all additions to naive strategy are necessary and drastically reduce the initial activation explosion.

Unshared Batch Normalization strategy therefore mitigates this exploding activation problem. This problem, leading to exploding gradient in our case, appears frequently in recurrent neural network. This suggests that future unrolled Resnets should use insights from research on recurrent networks optimization, including careful initialization (Henaff et al., 2016) and parametrization changes (Hochreiter & Schmidhuber, 1997).

5 CONCLUSION

We show that Resnets perform both representation learning and iterative refinement in different architectures and depending on depth. Our main contribution is formalizing the view of iterative refinement and showing analytically that residual blocks naturally encourage representations to move

in the half space of negative loss gradient, thus implementing a gradient descent in the activation space (each block reduces loss and improves accuracy).

Qualitatively we find that this mechanism helps correcting the predictions for *near misclassified* samples. In addition, we observe that Resnets can also learn to perform representation learning, especially in the absence of multiple compositional (convolution) layers in the main path of the network (Eg. single representation Resnet and pooling Resnet used for our analysis). But in general we find that the representation learning behavior tends to concentrate in the first few blocks while the rest of the higher blocks perform iterative refinement of features.

Finally, we surprisingly find that sharing residual blocks naively leads to overfitting. We show that this happens because of representation explosion. Empirical analysis shows that this problem is mitigated by using a variation of recurrent batch normalization with unshared parameters, which solves the problem by reducing the explosion. Iterative view suggests that top blocks of residual network could be fully shareable, and we leave this for future work. Additionally, the developed formal view could help explaining the success of other architectures using shortcut connections.

REFERENCES

- D. Arpit, Y. Zhou, B. U Kota, and V. Govindaraju. Normalization propagation: A parametric technique for removing internal covariate shift in deep networks. *ICML*, 2016.
- Tim Cooijmans, Nicolas Ballas, César Laurent, Çağlar Gülçehre, and Aaron Courville. Recurrent batch normalization. *arXiv preprint arXiv:1603.09025*, 2016.
- X. Glorot and Y. Bengio. Understanding the difficulty of training deep feedforward neural networks. In *Aistats*, 2010.
- K. Greff, R. Srivastava, and J. Schmidhuber. Highway and residual networks learn unrolled iterative estimation. *arXiv*, 2016.
- K. He, X. Zhang, S. Ren, and J. Sun. Delving deep into rectifiers: Surpassing human-level performance on imagenet classification. In *ICCV*, 2015.
- K. He, X. Zhang, S. Ren, and J. Sun. Deep residual learning for image recognition. In *CVPR*, 2016a.
- K. He, X. Zhang, S. Ren, and J. Sun. Identity mappings in deep residual networks. In *ECCV*, 2016b.
- M. Henaff, A. Szlam, and Y. LeCun. Recurrent orthogonal networks and long-memory tasks. In *ICML*, 2016.
- S. Hochreiter and J. Schmidhuber. Long short-term memory. *Neural computation*, 1997.
- Furong Huang, Jordan Ash, John Langford, and Robert Schapire. Learning deep resnet blocks sequentially using boosting theory. *arXiv preprint arXiv:1706.04964*, 2017.
- S. Ioffe and C. Szegedy. Batch normalization: Accelerating deep network training by reducing internal covariate shift. In *ICML*, 2015.
- A. Krizhevsky and G. Hinton. Learning multiple layers of features from tiny images. 2009.
- A. Krizhevsky, I. Sutskever, and G. Hinton. Imagenet classification with deep convolutional neural networks. In *NIPS*, 2012.
- Q. Liao and T. Poggio. Bridging the gaps between residual learning, recurrent neural networks and visual cortex. *arXiv*, 2016.
- E. Littwin and L. Wolf. The loss surface of residual networks: Ensembles and the role of batch normalization. *arXiv*, 2016.
- V. Nair and G. Hinton. Rectified linear units improve restricted boltzmann machines. In *ICML*, 2010.
- K. Simonyan and A. Zisserman. Very deep convolutional networks for large-scale image recognition. *arXiv*, 2014.

-
- S. Thorpe, D. Fize, and C. Marlot. Speed of processing in the human visual system. *Nature*, 1996.
- S. Vanmarcke, F. Calders, and F. Wagemans. The time-course of ultrarapid categorization: The influence of scene congruency and top-down processing. *i-Perception*, 2016.
- A. Veit, M. Wilber, and S. Belongie. Residual networks are exponential ensembles of relatively shallow networks. *arXiv*, 2016.

Appendices

A FURTHER ANALYSIS

A.1 A SIDE-EFFECT OF MOVING IN THE HALF SPACE OF $-\frac{\partial\mathcal{L}(\mathbf{h}_o)}{\partial\mathbf{h}_o}$

Let $\mathbf{h}_o = \mathbf{W}\mathbf{x} + \mathbf{b}$ be the output of the first layer (convolution) of a ResNet. In this analysis we show that if \mathbf{h}_o moves in the half space of $-\frac{\partial\mathcal{L}(\mathbf{h}_o)}{\partial\mathbf{h}_o}$, then it is equivalent to updating the parameters of the convolution layer using a gradient update step. To see this, consider the change in \mathbf{h}_o from updating parameters using gradient descent with step size η . This is given by,

$$\Delta\mathbf{h}_o = (\mathbf{W} - \eta\frac{\partial\mathcal{L}}{\partial\mathbf{W}})\mathbf{x} + (\mathbf{b} - \eta\frac{\partial\mathcal{L}}{\partial\mathbf{b}}) - (\mathbf{W}\mathbf{x} + \mathbf{b}) \quad (5)$$

$$= -\eta\frac{\partial\mathcal{L}}{\partial\mathbf{W}}\mathbf{x} - \eta\frac{\partial\mathcal{L}}{\partial\mathbf{b}} \quad (6)$$

$$= -\eta\frac{\partial\mathcal{L}}{\partial\mathbf{h}_o} \left(\frac{\partial\mathbf{h}_o}{\partial\mathbf{W}}\mathbf{x} + \frac{\partial\mathbf{h}_o}{\partial\mathbf{b}} \right) \quad (7)$$

$$= -\eta\frac{\partial\mathcal{L}}{\partial\mathbf{h}_o} (\|\mathbf{x}\|^2 + 1) \quad (8)$$

$$\propto -\frac{\partial\mathcal{L}}{\partial\mathbf{h}_o} \quad (9)$$

Thus, moving \mathbf{h}_o in the half space of $-\frac{\partial\mathcal{L}}{\partial\mathbf{h}_o}$ has the same effect as that achieved by updating the parameters \mathbf{W} , \mathbf{b} using gradient descent. Although we found this insight interesting, we don't build upon it in this paper. We leave this as a future work.

B ANALYSIS ON CIFAR-100

Here we report the experiments as done in sections 4.1 and 4.2, for CIFAR-100 dataset. The plots are shown in figures 10, 11 and 12. The conclusions are same as reported in the main text for CIFAR-10.

C ANALYSIS OF INTERMEDIATE METRICS ON CIFAR-10 AND CIFAR-100

Here we plot the accuracy, cosine loss and ℓ^2 ratio metrics corresponding to each individual residual block on validation during the training process for CIFAR-10 (figures 13, 14, 5) and CIFAR-100 (figures 15, 16, 17). These plots are recorded only for the residual blocks in the last space for each architecture (this is because otherwise the dimensions of the output of the residual block and the classifier will not match). In the case of cosine loss after individual residual block, this set of experiments is achieved by plugging the classifier right after each hidden representation and measuring the cosine between the gradient w.r.t. hidden representation and the corresponding residual block's output.

We find that the accuracy after individual residual blocks increases gradually as we move from lower to higher residual blocks. Cosine loss on the other hand consistently remains negative for all architectures. Finally ℓ^2 ratio tends to increase for residual blocks as training progresses.

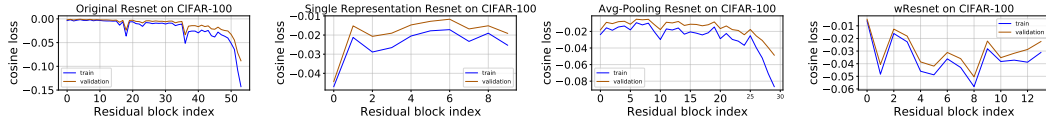


Figure 10: Average cos loss between residual block $F(\mathbf{h}_i)$ and $\frac{\partial \mathcal{L}(\mathbf{h}_i)}{\partial \mathbf{h}_i}$ for (left to right) original Resnet, single representation Resnet, avg-pooling Resnet, and wideResnet on CIFAR-100.

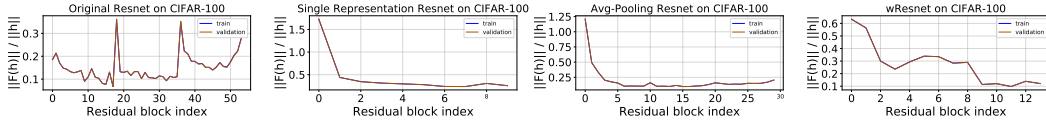


Figure 11: Average ratio of ℓ^2 norm of output of residual block to the norm of the input of residual block for (left to right) original Resnet, single representation Resnet, avg-pooling Resnet, and wideResnet on CIFAR-100. (Train and validation curves are overlapping.)

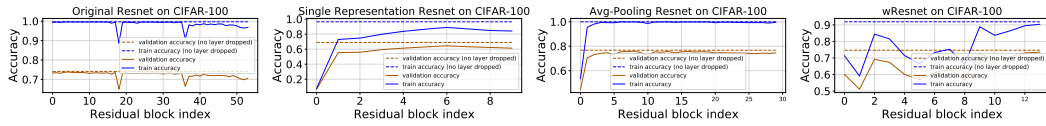


Figure 12: Final prediction accuracy when individual residual blocks are dropped for (left to right) original Resnet, single representation Resnet, avg-pooling Resnet, and wideResnet on CIFAR-100.

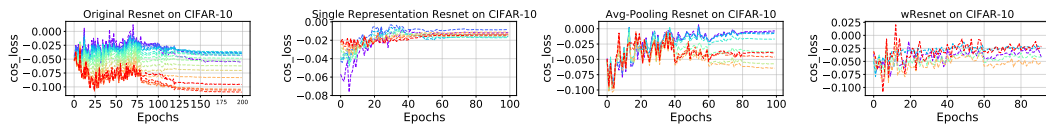


Figure 13: Average cos loss between residual block $F(\mathbf{h}_i)$ and $\frac{\partial \mathcal{L}(\mathbf{h}_i)}{\partial \mathbf{h}_i}$ during training for (left to right) original Resnet, single representation Resnet, avg-pooling Resnet, and wideResnet on CIFAR-10. (Blue to red spectrum denotes lower to higher residual blocks)

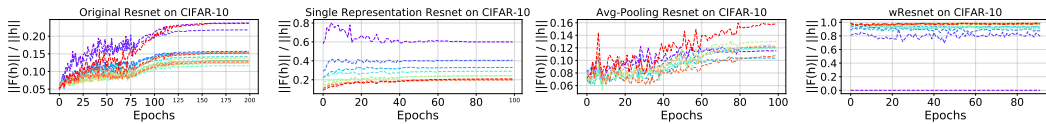


Figure 14: Average ratio of ℓ^2 norm of output of residual block to the norm of the input of residual block during training for (left to right) original Resnet, single representation Resnet, avg-pooling Resnet, and wideResnet on CIFAR-10. (Blue to red spectrum denotes lower to higher residual blocks)

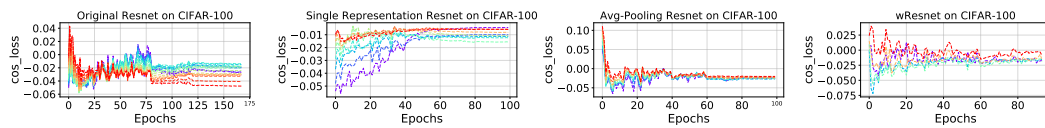


Figure 15: Average cos loss between residual block $F(\mathbf{h}_i)$ and $\frac{\partial \mathcal{L}(\mathbf{h}_i)}{\partial \mathbf{h}_i}$ during training for (left to right) original Resnet, single representation Resnet, avg-pooling Resnet, and wideResnet on CIFAR-100. (Blue to red spectrum denotes lower to higher residual blocks)

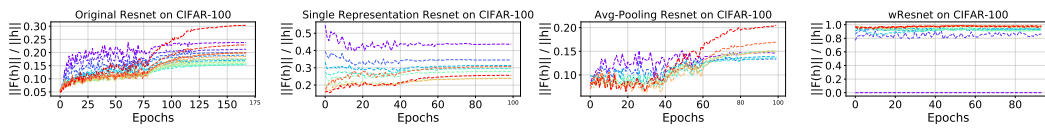


Figure 16: Average ratio of ℓ^2 norm of output of residual block to the norm of the input of residual block during training for (left to right) original Resnet, single representation Resnet, avg-pooling Resnet, and wideResnet on CIFAR-100. (Blue to red spectrum denotes lower to higher residual blocks)

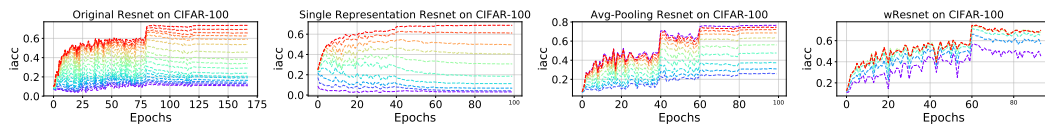


Figure 17: Prediction accuracy when plugging classifier after hidden states in the last stage of Resnets(if any) during training for (left to right) original Resnet, single representation Resnet, avg-pooling Resnet, and wideResnet on CIFAR-100. (Blue to red spectrum denotes lower to higher residual blocks)